

## RESEARCH ARTICLE

View Article Online  
View Journal

Cite this: DOI: 10.1039/d6qo00263c

# Supramolecular masks for the regioselective synthesis of Diels–Alder hetero-tris-adduct C<sub>60</sub> fullerene

Cristina Castanyer,  † Tània Pèlachs,  † Elias A. Romero-Cavagnaro,   
Clara Sabrià,  Ferran Feixas,  Xavi Ribas,  \* Anna Roglans  \* and  
Anna Pla-Quintana  \*

Herein, we report the regioselective hetero-tris-functionalization of fullerenes *via* a sequential Diels–Alder cycloaddition strategy. The first addend is introduced onto C<sub>60</sub> through a cascade process involving a Ru-catalyzed cycloisomerization of 1,6-enynes, followed by a Diels–Alder reaction with C<sub>60</sub>. Subsequently, supramolecular nanocapsules are employed as regioselective masks, enabling enhanced control over the formation of a hetero-tris-adduct bearing two pentacene units. These units are positioned equatorially with respect to the initial addend and adopt a *trans*-1 relative orientation. Notably, a single pure tris-regioisomer, *e,e,t*(1), is obtained for both **2a-Pn<sub>2</sub>** and **2d-Pn<sub>2</sub>**. Access to pure-isomer hetero-tris Diels–Alder adducts is unprecedented and highlights the broad potential of the supramolecular mask strategy.

Received 2nd March 2026,

Accepted 3rd April 2026

DOI: 10.1039/d6qo00263c

rsc.li/frontiers-organic

## Introduction

Interest in C<sub>60</sub> has grown considerably since the first large-scale production of this compound thirty-five years ago.<sup>1</sup> In order to enhance the utility and broaden the applications of fullerenes, they need to be functionalized.<sup>2</sup> Structural modifications by introducing specific functional groups serve multiple purposes, including enhancing solubility in organic solvents, which is crucial for solution-based processing in materials science, and improving solubility in water, a key factor for biomedical applications.<sup>3</sup> Moreover, by introducing specific functional groups, the electronic properties of the fullerene cage can be fine-tuned, thereby improving photovoltaic performance in organic and perovskite solar cells.<sup>4</sup>

Nowadays, highly efficient synthetic methods are available to introduce a single addend into pristine C<sub>60</sub>. The Diels–Alder (DA) cycloaddition reaction, in particular, has been widely used to synthesize a large number of fullerene derivatives in which the fullerene molecule behaves as a dienophile due to the electron-deficient nature of its [6,6] bonds.<sup>5</sup> The Diels–Alder cycloaddition can proceed either with a preformed diene or *via in situ* generation of the diene from unsaturated substrates through a transition metal-catalysed cycloisomeriza-

tion.<sup>6</sup> This latter strategy allows for the diversification of both functional groups and scaffolds that can be attached to the fullerene.

However, once the first addend is attached to the fullerene cage, 9 different [6,6] bonds remain available for a second addition and, considering a threefold addition, the number of theoretically possible regioisomers increases from 9 to 46. This growing complexity makes it increasingly difficult to isolate pure isomers, complicating their practical applications in the targeted fields. Moreover, isolating these regioisomeric mixtures typically requires multistep high-performance liquid chromatography, which is a costly, labour-intensive, and time-consuming process that often proves impractical. Therefore, since properties of the resulting adducts are largely determined by the addition site on the fullerene cage, new approaches are needed to achieve controlled poly-functionalization of fullerenes, enhancing itero-, chemo-, regio-, and stereoselectivity to limit the formation of unwanted isomers.

Among these multiple addition products, tris-adducts are of special interest. In the area of solar energy conversion, they often exhibit higher LUMO energy levels than their mono- or bis-substituted counterparts, which can enhance performance in organic solar cells.<sup>7</sup> Additionally, the *e,e,e* trismalonate fullerene derivative<sup>8</sup> exhibits pronounced water solubility, enhancing its suitability for biomedical applications, particularly as an antioxidant agent with potential use in treating degenerative diseases.<sup>9</sup> In material science, the presence of three functional sites can also afford the construction of

Institut de Química Computacional i Catalisi (IQCC) and Departament de Química, Universitat de Girona, M. Aurèlia Capmany, 69, 17003 Girona, Catalonia, Spain.  
E-mail: anna.plaq@udg.edu, anna.roglans@udg.edu, xavi.ribas@udg.edu

† Equally contributing author.



complex architectures, including dendrimers<sup>10</sup> and polymers. In a particular case, a self-assembly ultrathin film made from a C<sub>60</sub> triscarboxylate ion and diazoresin showed good load-bearing and lubricating properties.<sup>11</sup>

The first powerful methodology for the regioselective synthesis of selected tris-adducts of C<sub>60</sub> was the tether-directed remote functionalization approach<sup>12</sup> pioneered by Diederich *et al.*<sup>13</sup> Given the limited number of methods available for accessing tris-functionalized adducts, this strategy marked a breakthrough. The use of tethered addend systems, whether with permanent or temporary tethers, has enabled relatively easy access to otherwise highly disfavoured addition patterns. One option is through the introduction of a temporary tether that blocks certain positions and directs the tris-functionalization, especially the Bingel reaction, towards specific positions on the fullerene.<sup>14</sup> Another option is the use of tripodal tethers, which, depending on their length and rigidity, directly guide the tris-functionalization to occur at only three defined bonds on the fullerene.<sup>15</sup>

An alternative, promising strategy is based on the use of supramolecular receptors as functionalization platforms for fullerenes. Our pioneering Supramolecular Mask Strategy (SMS),<sup>16</sup> *i.e.* using encapsulated fullerenes in supramolecular nanocapsules, targets the synthesis of isomer-pure poly-functionalized fullerenes, and consists of a regioselective fullerene functionalization technique in which a host molecule, exhibiting a high affinity for the fullerene guest, shields part of the fullerene surface, unveiling the sites exposed and available for chemical modification (Fig. 1a). The SMS was initially applied to C<sub>60</sub> in combination with the Bingel reaction, affording the

pure *e,e,e,e* tetrakis-Et<sub>4</sub>-C<sub>60</sub> adduct.<sup>16a</sup> Furthermore, the SMS was expanded for the Diels–Alder reaction, leading to the selective formation of the *e,e* bis-An<sub>2</sub>-C<sub>60</sub>.<sup>16b</sup> Upon increasing the acene to pentacene, the *trans*-1 bis-Pn<sub>2</sub>-C<sub>60</sub> was obtained. These DA-adducts were subsequently subjected to the SMS under Bingel conditions to access hetero-tris-adducts through the combination of two distinct reactions. We hypothesised that Diels–Alder cycloaddends could be used as a handle to obtain tris-adducts of C<sub>60</sub> as regioisomerically pure adducts under the SMS. Hence, we describe in this work the regioselective hetero-tris-functionalization of fullerene using Diels–Alder cycloadditions in a sequential strategy. A first addend is introduced onto the fullerene through a cascade process involving a Ru-catalyzed cycloisomerization of 1,6-enynes followed by a Diels–Alder reaction with C<sub>60</sub>. Subsequently, nanocapsules are employed as supramolecular masks to obtain high levels of regioselectivity towards a hetero-tris-adduct containing two pentacene units positioned equatorially with respect to the initial addend and adopting a *trans*-1 relative orientation (Fig. 1b). The access to pure-isomer hetero-tris-DA-adducts is unprecedented and shows the broad potential of the supramolecular mask strategy.

## Results and discussion

### Synthesis and encapsulation of the mono-adducts 2

We have worked extensively on the development of cascade processes to obtain monofunctionalized fullerene and fulleroid derivatives.<sup>6f,g,h,i</sup> In this context, we turned our attention to the preparation of a series of non-symmetric mono-cycloadducts **2a–2e** by a cascade process encompassing a Ru-catalyzed cycloisomerization of 1,6-enynes **1a–1e** followed by a Diels–Alder reaction with C<sub>60</sub>. Although the Ru-catalyzed cycloisomerization of 1,6-enynes is well established and known to afford 1,3-dienes,<sup>17</sup> it has never been applied to generate a diene, either *in situ* or in isolated form, that subsequently reacts with C<sub>60</sub>. With this unexplored reactivity as a target, we selected the cascade reaction between NTs-tethered enyne **1a** and pristine fullerene under ruthenium catalysis as a model system for optimization (see Table S1). The best reaction conditions were found to be 2.2 equivalents of the 1,6-enyne **1**, 1 equivalent of C<sub>60</sub>, using a 10 mol% of Grubbs 1<sup>st</sup> generation catalyst in *o*-DCB at 90 °C.

The scope of the process is shown in Scheme 1. The reaction displayed a broad substrate scope and proceeded efficiently with both aryl/heteroaryl and alkyl substituents on the alkyne terminus of the enyne. Electron-donating groups in the phenyl ring gave good yields (**2a**, 53% yield), whereas strong electron-withdrawing substituents reduced the efficiency (**2b**, 24% yield). Notably, thiophenyl (**2c**, 52% yield) and alkyl alkynes (**2d**, 64% yield) were well tolerated, providing good yields, and modification of the tether (tosyl *vs.* *tert*-butyl malonate) maintained the reactivity, affording a 36% yield of the corresponding product **2e**.

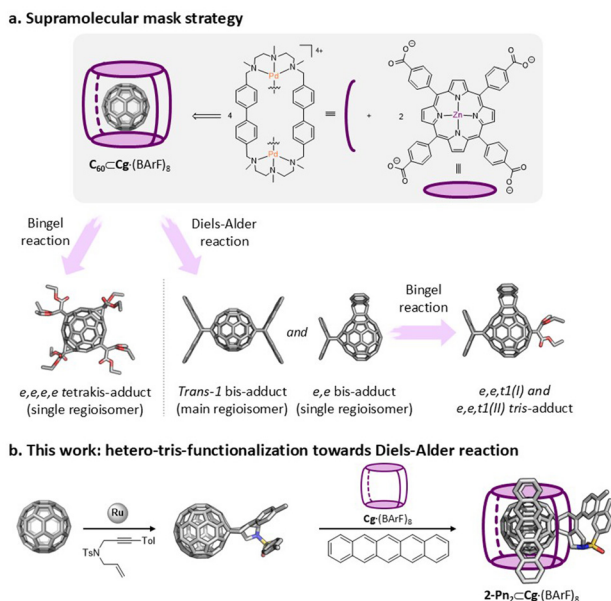
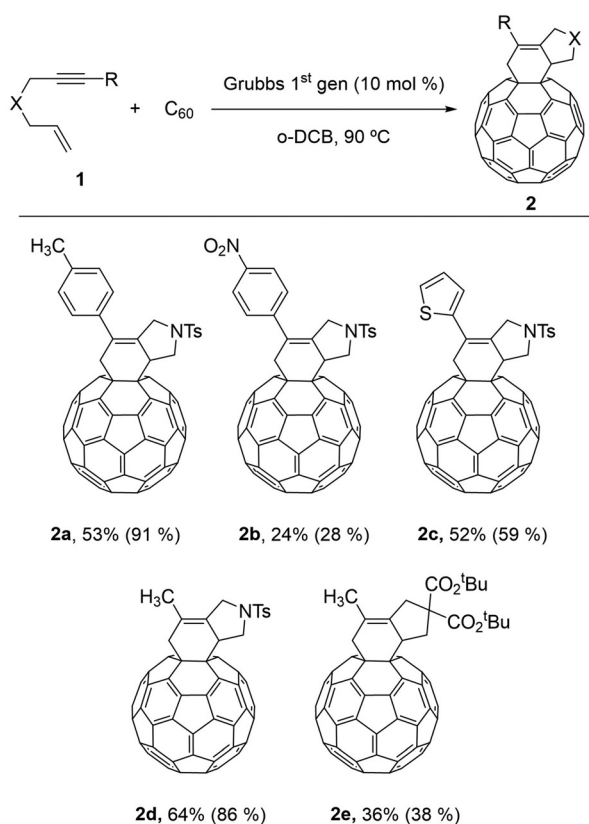


**Fig. 1** (a) Schematic representation of the synthesis of the reported tetragonal prismatic Cg·(BARF)<sub>8</sub> cage and its application in the functionalization of C<sub>60</sub>, obtaining pure regio-isomers. (b) Schematic representation of this work: hetero-tris-functionalization of C<sub>60</sub> by Diels–Alder cycloadditions in a sequential strategy.





**Scheme 1** Synthesis of compounds 2a–2e by cycloaddition of enynes 1 with C<sub>60</sub>. The values in parentheses are the yields based on the amount of C<sub>60</sub> consumed.

Based on their structural differences, three of the mono-derivatives 2a, 2d and 2e were selected to attempt the SMS-based Diels–Alder functionalization with pentacene. First, the host–guest complexes were prepared by adding two equivalents of a toluene solution of the mono-derivative 2 to an acetonitrile solution of the Cg·(BARF)<sub>8</sub> cage, maintaining a solvent ratio of 4:1 toluene:acetonitrile. After 24 hours of reaction, the HRMS analysis confirmed the quantitative formation of the host–guest complex (Fig. S23–S25).

#### Diels–Alder reaction with pentacene on the 2a mono-adduct

We first focused on the regiofunctionalization of 2a with pentacene. The reaction was carried out under the following conditions: 65 °C, 24 h, cage concentration of 10<sup>−3</sup> M, acetonitrile (MeCN):dichloromethane (DCM) (3:1) solvent mixture, and under N<sub>2</sub> atmosphere in the dark (Fig. 2a). Upon addition of 1.5 equivalents of pentacene, the reaction evolved towards the formation of a mixture of bis- and tris-adducts. Increasing the amount of pentacene up to 2.2 equivalents likewise led mainly to tris-adduct formation, albeit with low amounts of bis-adducts detected by HRMS (Fig. 2b and S26).

Upon completion of the reaction, the release of the functionalized fullerenes from the nanocapsule was then investigated. Initially, a solvent-washing protocol was attempted, which was

expected to leave the empty cage in the solid state, fully releasing the encapsulated fullerenes into solution; this involved suspending the host–guest complex in CS<sub>2</sub>, followed by sonication. Under these conditions, the cage indeed remained in the solid, and fullerene release was observed. However, HRMS analysis of the recovered cage still revealed a major peak corresponding to the encapsulated tris-adduct. Consequently, an acid-mediated strategy was selected to disassemble the nanocapsule and ensure the complete liberation of the guest. Hence, trifluoromethanesulfonic acid was added to the acetonitrile solution of the cage, after which the fullerenes were recovered by extractions with toluene.

After the release of the functionalized fullerenes, the reaction crude was initially analysed by HPLC. The resulting chromatogram displayed a predominant peak (Fig. 2c and S27; R<sub>t</sub> = 9.70 min) together with several minor peaks, indicative of the formation of multiple regioisomers. To unravel the nature of the main peak, the crude mixture was purified by preparative thin-layer chromatography using toluene as eluent. The isolated product was subsequently reinjected into the HPLC, confirming its correspondence to the major peak through an identical absorption profile (Fig. 2e). The isolated yield was determined to be 56.7% by HPLC analysis, using the C<sub>60</sub> as an internal standard.

The HRMS analysis confirmed that the C<sub>60</sub> derivative incorporates two pentacene units in addition to the initially installed single substituent (Fig. S32). Structural characterization of the isolated hetero-tris-adduct by NMR spectroscopy revealed that the two pentacene units occupy *equatorial* positions with respect to the mono-addend 2a and adopt a *trans*-1 relative arrangement among them (full characterization in S28–S31). According to this *e,e,t1* substitution pattern, two distinct isomers, denoted *e,e,t1(I)* and *e,e,t1(II)*, are in principle possible (Fig. 2d), in agreement with previous reports on related systems.<sup>16a</sup> Careful analysis of the NMR spectra, together with conformational analysis of the fullerene-cage adduct, showed the formation of only one isomer, which was assigned to *e,e,t1(I)*. In the 5–6 ppm region of the <sup>1</sup>H-NMR spectrum, four singlets integrating one proton each are observed and assigned to the C<sub>sp3</sub> protons of the reacted pentacene moieties. Two of these protons are oriented towards the mono-addend of 2a and present different chemical shifts as a consequence of the stereocenter in the mono-addend, which renders them inequivalent. The remaining two protons are oriented towards the non-functionalized surface of the C<sub>60</sub> and display closely spaced yet distinguishable resonances. Furthermore, NOESY experiments show no cross-peaks between the aromatic protons of the pentacene units and those of the phenyl of the 2a addend. This observation is consistent with the *e,e,t1(I)* isomer, in which these protons are not in close spatial proximity; in contrast, the *e,e,t1(II)* isomer would be expected to exhibit such cross-peaks.

The sole formation of the *e,e,t1(I)* isomer can be rationalized by considering the orientation of 2a addends within the Cg·(BARF)<sub>8</sub> nanocapsule. Encapsulation allows two possible orientations of the C–C bond linking the addend of 2a to the



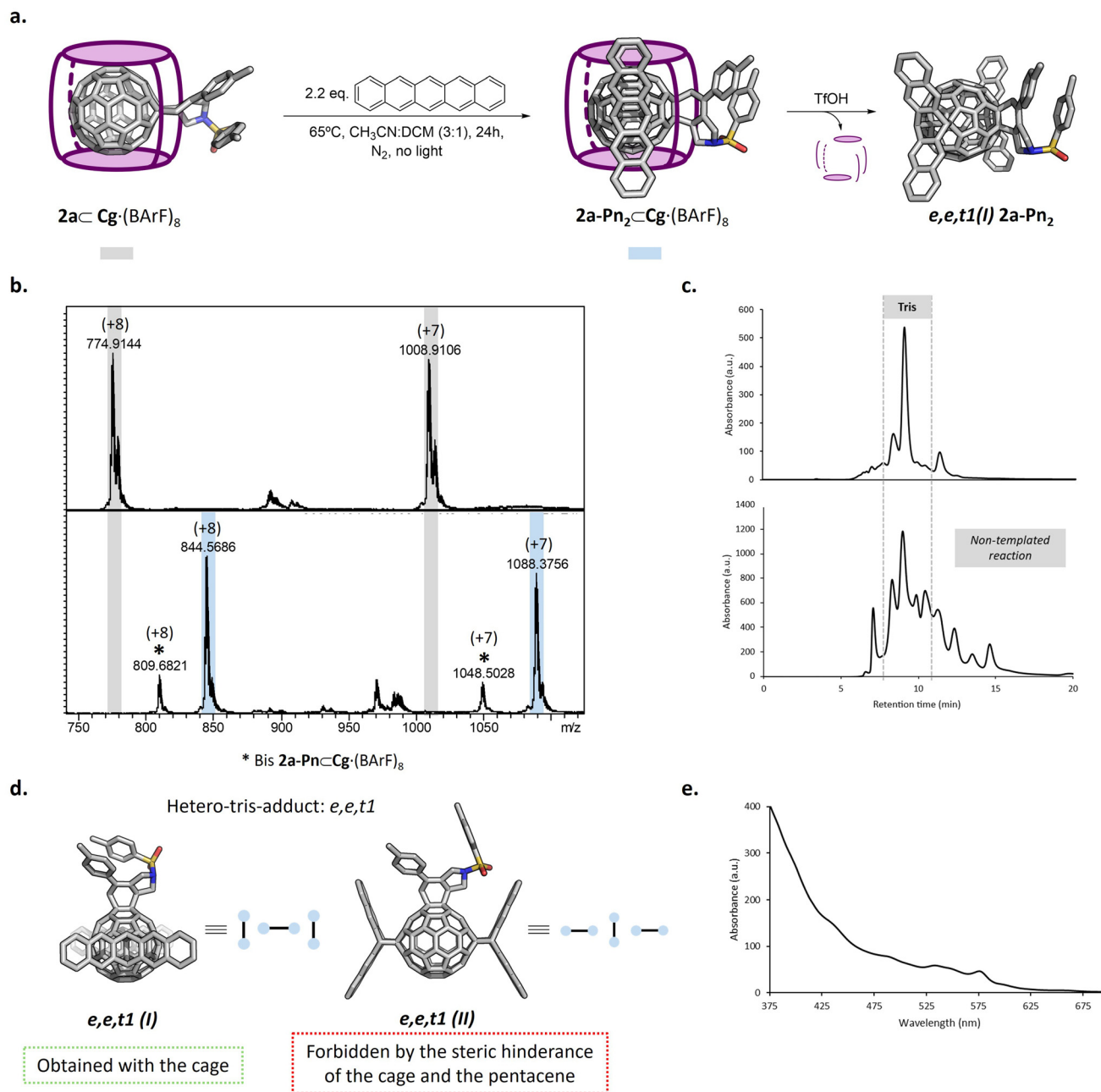


**Fig. 2** (a) Synthesis of the hetero-tris-adduct *e,e,t1(I)* **2a-Pn<sub>2</sub>**. (b) HRMS monitoring of the formation of *e,e,t1(I)* **2a-Pn<sub>2</sub>**. (c) HPLC of the reaction crude in the presence of the nanocapsule (top) and in the absence of the nanocapsule (bottom). (d) Representation of the two possible isomers of the **2a-Pn<sub>2</sub>**. (e) Absorption spectrum of the isolated *e,e,t1(I)* **2a-Pn<sub>2</sub>**.

$C_{60}$  core, namely vertical or horizontal with respect to the porphyrin panels of the cage. When the bond adopts a vertical orientation, the two *equatorial* bonds exposed through the contiguous gates are oriented horizontally, thereby enabling the incoming pentacene units to approach in a vertical orientation that minimizes steric clashes with the cage, as was previously demonstrated in studies of Diels–Alder di-functionalization of the  $C_{60}$ .<sup>16b</sup> In contrast, when the mono-addend is oriented horizontally, the *equatorial* bonds exposed through adjacent gates are vertical, which hinders the approach of pentacene in

a horizontal orientation relative to the porphyrin units and is therefore sterically disfavoured. Consequently, the nanocapsule exclusively promotes the formation of the *e,e,t1(I)* isomer, effectively directing the reaction toward a single isomer. This assignment is also in agreement with the Molecular Dynamics simulations of the encapsulated **2a-Cg·(BARF)<sub>8</sub>** (Fig. S43).

To assess the role of the cage in controlling the reaction outcome, a control experiment was performed by conducting the Diels–Alder reaction of pentacene with mono-adduct **2a** in the absence of the cage. Owing to the poor solubility of the



fullerene in acetonitrile (the solvent used with the reaction inside the cage), the reaction was carried out in toluene while maintaining identical reaction conditions. HPLC analysis of the crude reaction mixture revealed a complex profile, with multiple peaks corresponding to a mixture of poly-adducts and their regioisomers (Fig. 2c bottom and Fig. S33). Notably, in the absence of the cage, the mono-adduct **2a** is still present, and a significantly higher proportion of poly-adducts is observed, together with a much broader distribution of regioisomers. These results highlight the key role of the cage as a supramolecular mask, enabling control over both the number of substituents added to the fullerene surface and the regioselectivity of the fullerene modification.

### Diels–Alder reaction with pentacene on the **2d** mono-adduct

The same reaction protocol was subsequently applied to a second selected mono-adduct, *i.e.* **2d**. The reaction was carried out using 2.2 eq. of pentacene at 65 °C, with a cage concentration of  $10^{-3}$  M in a MeCN : DCM (3 : 1) solvent mixture under  $N_2$  atmosphere in the dark (Fig. 3a). HRMS monitoring revealed that after 24 hours, the bis-adduct was the predominant species. Upon extending the reaction time to 48 hours, only trace amounts of the bis-adduct remained, while the corresponding tris-adduct was identified as the major product (Fig. S34).

Following nanocapsule disassembly and work-up, HPLC analysis displayed a main peak, whose absorption spectrum is consistent with the *e,e,t1(I)* tris-adduct, along with additional peaks corresponding to other functionalized fullerenes patterns (Fig. 3b, d and S35; main peak at  $R_t = 9.7$  min, other peaks:  $R_t = 10.8$  and 8.8 min). No unreacted **2d** mono-adduct was detected. Purification of the main product was successful, affording the tris-adduct **2d-Pn<sub>3</sub>** in a 38% isolated yield, determined by HPLC using  $C_{60}$  as internal standard. HPLC and absorption analysis of the isolated tris-adduct show spectral features comparable to those of *e,e,t1(I)* **2a-Pn<sub>3</sub>** (Fig. S27 and S35).

The isolated tris-adduct was further characterized by  $^1H$ -NMR spectroscopy (Fig. 3c and full characterization at S36 and S37). The pattern of the  $C_{sp^3}$  protons of the pentacene moiety exhibits a 2 : 1 : 1 splitting rather than the expected 1 : 1 : 1 : 1, likely due to overlap of two proton signals, as suggested by the observed broad peak. Nevertheless, since both products obtained from **2a** and **2d** display identical absorption spectra, indicating identical substitution pattern on  $C_{60}$ , this isomer is assigned as *e,e,t1(I)* **2d-Pn<sub>3</sub>**.

Similarly, as in **2a**, a control experiment was performed by reacting **2d** with pentacene in the absence of the cage (in toluene due to the insolubility of **2d** in acetonitrile). HPLC analysis of the reaction crude revealed multiple peaks (Fig. 3b bottom and S40), indicating a lack of selectivity with respect to both the number of pentacene moieties added and the formation of a mixture of regioisomers.

### Diels–Alder reaction with pentacene on the **2e** mono-adduct

The last compound to which we applied the SMS was **2e**. The reaction conditions were analogous to those used for **2d**.

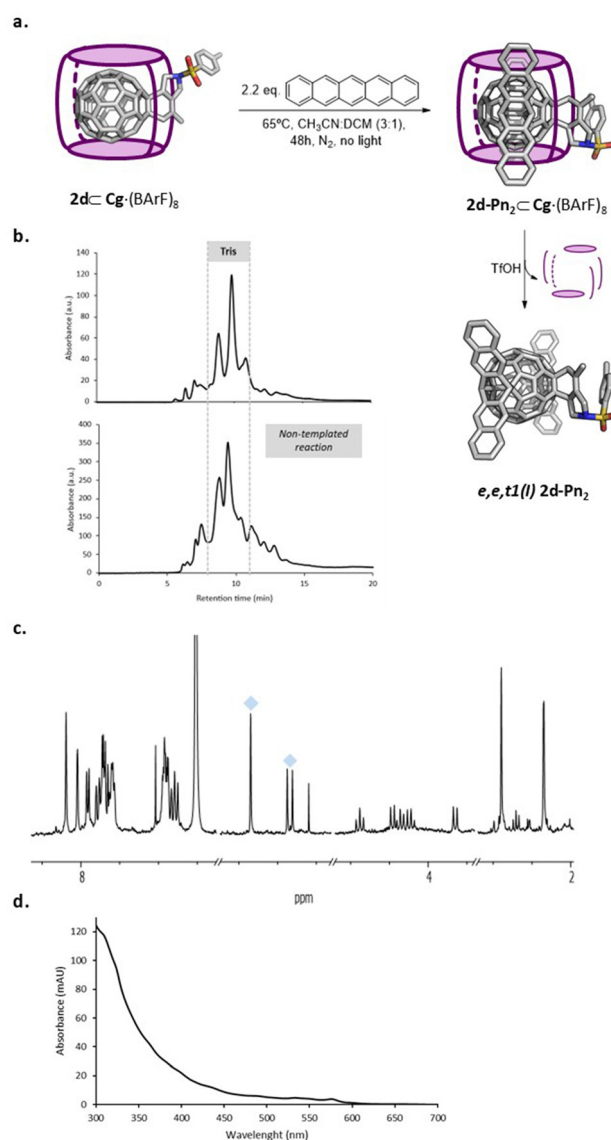


**Fig. 3** (a) Synthesis of the hetero-tris-adduct *e,e,t1(I)*-**2d-Pn<sub>3</sub>**. (b) HPLC of the reaction crude in the presence of the nanocapsule (top) and in the absence of the nanocapsule (bottom). (c)  $^1H$ -NMR spectrum of the isolated *e,e,t1(I)* **2d-Pn<sub>3</sub>**. Peaks of the  $C_{sp^3}$ -H of the pentacene are labelled with a blue rhombus. (d) Absorption spectrum of the isolated *e,e,t1(I)* **2d-Pn<sub>3</sub>**.

HRMS monitoring indicated that, after 48 hours, the tris-adduct was identified as the major product (Fig. S41).

Following nanocapsule disassembly and workup, the crude mixture was analysed by HPLC, revealing five distinct peaks (Fig. S42). These were assigned, from longest to shortest retention time, as follows: (i) is unassigned, which was already present in the starting mono-adduct (as observed in the HPLC of the mono-adduct); (ii) a small amount of unreacted mono-adduct; (iii and iv) two new peaks at 8.9 min and 7.8 min, both displaying absorption patterns consistent with functionalized fullerenes, and (v) pentacene. Attempts to isolate the tris-adduct were hampered due to strong interactions between the



fullerenes and silica. Unexpectedly, the extraction of fullerene species from silica was challenging, yielding only small recoverable quantities of degraded compounds. Nevertheless, HRMS analysis of the reaction crude suggests a similar control of the regioselectivity in the tris-adduct product formed.

## Conclusions

In summary, the selective hetero-tris-functionalization of fullerene using Diels–Alder cycloadditions in a sequential strategy is achieved. A first addend is introduced onto the fullerene through a cascade process involving a Ru-catalyzed cycloisomerization of 1,6-enynes followed by a Diels–Alder reaction with C<sub>60</sub>. Subsequently, nanocapsules are employed as supramolecular masks to obtain higher levels of regioselectivity towards a Diels Alder hetero-tris-adduct containing two pentacene units positioned *equatorially* with respect to the initial addend and in a *trans-1* relative orientation. In this manner, pure tris-regioisomers *e,e,t1(I)* **2a-Pn**<sub>2</sub> and *e,e,t1(I)* **2d-Pn**<sub>2</sub> are obtained in good yields. The nature of the initial substituent in **2** influences the formation of the hetero-tris-adducts: bulkier addends (**2a** > **2d**) provide improved regioselective control, favouring the formation of the *e,e,t1(I)* isomer while minimizing other hetero-tris-adducts. Moreover, **2a** forms the corresponding hetero-tris-adduct within 24 hours, whereas **2d** and **2e** require 48 hours to achieve comparable formation. This behaviour is attributed to the stronger confinement of the bulkier mono-adduct within the C<sub>g</sub>-(BARF)<sub>8</sub> cage, which facilitates a more efficient and regioselective addition of pentacene. Overall, the cage enables control over both the degree of functionalization of the fullerene surface and the regioselectivity of the addition. Access to pure-isomer hetero-tris-DA-adducts is unprecedented and demonstrates the broad potential of the supramolecular mask strategy.

## Author contributions

The manuscript was written with contributions from all authors. All authors have approved the final version of the manuscript.

## Conflicts of interest

There are no conflicts to declare.

## Data availability

The data supporting this article have been included as part of the supplementary information (SI). Supplementary information: detailed synthetic procedures and complete characterization data for all new compounds. See DOI: <https://doi.org/10.1039/d6qo00263c>.

## Acknowledgements

This work was supported by projects PID2022-136970NB-I00 (to X. R.), PID2023-146849NB-I00 (to A. P.-Q.), PID2022-141676NB-I00 (to F. F.), RYC2020-029552-I (to F. F.), and TED2021-130573B-I00 (to X. R.) funded by the Ministerio de Ciencia, Innovación y Universidades of Spain MCIU/AEI/10.13039/501100011033 and FEDER, UE, and projects 2021SGR00475, 2021-SGR-00487, and 2021-SGR-623 funded by Generalitat de Catalunya. C. C. thanks MINECO for a FPI predoctoral grant, T. P. thanks MINECO for a FPU-PhD grant, E. R. thanks Generalitat de Catalunya for a FI-2024 Joan Oró predoctoral grant, and C. S. thanks UdG for an IF-PhD grant. X. R. is also grateful for an ICREA Academia award.

## References

- (a) H. W. Kroto, J. R. Heath, S. C. O'Brien, R. F. Curl and R. E. Smalley, C<sub>60</sub>: Buckminsterfullerene, *Nature*, 1985, **318**, 162–163; (b) W. Krätschmer, L. D. Lamb, K. Fostiropoulos and D. R. Huffman, Solid C<sub>60</sub>: a new form of carbon, *Nature*, 1990, **347**, 354–358.
- (a) A. Hirsch, *The Chemistry of the Fullerenes*, Thieme, Stuttgart, 1994; (b) F. Diederich and M. Gómez-López, Supramolecular fullerene chemistry, *Chem. Soc. Rev.*, 1999, **28**, 263–277; (c) X. Lu, T. Akasaka and Z. Slanina, *Handbook of Fullerene Science and Technology*, Springer Nature, Singapore, 1st edn, 2022; (d) Y. R. Yao, O. Fernandez-Delgado and L. Echegoyen, Fullerenes and their applications, in *Handbook of Carbon-Based Nanomaterials*, ed. S. Thomas, C. Sarathchandran, S. A. Ilangovan and J. C. Moreno-Piraján, Elsevier, Amsterdam, 2021, pp. 19–158; (e) *Chemical Functionalization of Carbon Nanomaterials*, ed. V. K. Thakur and M. K. Thakur, CRC Press, Boca Raton, FL, 1st edn, 2015.
- (a) R. Biswas, C. Batista Da Rocha, R. A. Bennick and J. Zhang, Water-soluble fullerene monoderivatives for biomedical applications, *ChemMedChem*, 2023, **18**, e202300296; (b) E. Castro, A. H. Garcia, G. Zavala and L. Echegoyen, Fullerenes in biology and medicine, *J. Mater. Chem. B*, 2017, **5**, 6523–6535; (c) F. Cataldo and T. Da Ros, in *Medicinal Chemistry and Pharmacological Potential of Fullerenes and Carbon Nanotubes*, ed. F. Cataldo and T. Da Ros, Springer Netherlands, Dordrecht, 2008; vol. 1; (d) N. Panwar, A. M. Soehartono, K. K. Chan, S. Zeng, G. Xu, J. Qu, P. Coquet, K. T. Yong and X. Chen, Nanocarbons for biology and medicine: sensing, imaging, and drug delivery, *Chem. Rev.*, 2019, **119**, 9559–9656; (e) J. Ramos-Soriano, J. J. Reina, B. M. Illescas, N. de la Cruz, L. Rodríguez-Pérez, F. Lasala, J. Rojo, R. Delgado and N. Martín, Synthesis of highly efficient multivalent disaccharide/[60]fullerene nanoballs for emergent viruses, *J. Am. Chem. Soc.*, 2019, **141**, 15403–15412; (f) C. Castanyer, Ç. Çelik, A. Roglans, A. Pla-Quintana, A. J. Stasyuk, Y. Yamakoshi and M. Solà, Enhancement of photoinduced



- reactive oxygen species generation in open-cage fullerenes, *Chem. Sci.*, 2025, **16**, 2673–2681.
- 4 (a) S. Collavini and J. L. Delgado, Fullerenes: the stars of photovoltaics, *Sustainable Energy Fuels*, 2018, **2**, 2480–2493; (b) L. Jia, M. Chen and S. Yang, Functionalization of fullerene materials toward applications in perovskite solar cells, *Mater. Chem. Front.*, 2020, **4**, 2256–2282; (c) O. Fernandez-Delgado, P. S. Chandrasekhar, N. Cano-Sampaio, Z. C. Simon, A. R. Puente-Santiago, F. Liu, E. Castro and L. Echegoyen, The role of fullerene derivatives in perovskite solar cells: electron transporting or electron extraction layers?, *J. Mater. Chem. C*, 2021, **9**, 10759–10767; (d) M. Izquierdo, B. Platzer, A. J. Stasyuk, O. A. Stasyuk, A. A. Voityuk, S. Cuesta, M. Solà, D. M. Guldi and N. Martín, All-fullerene electron donor-acceptor conjugates, *Angew. Chem., Int. Ed.*, 2019, **58**, 6932–6937.
- 5 (a) W. Sliwa, Diels-Alder reactions of fullerenes, *Fullerene Sci. Technol.*, 1997, **5**, 1133–1175; (b) N. Martín, J. L. Segura and F. Wudl, New Concepts in Diels-Alder Cycloadditions to Fullerenes, in *Fullerenes: From Synthesis to Optoelectronic Properties, Developments in Fullerene Science*, ed. D. M. Guldi and N. Martín, Springer, Dordrecht, 2002, vol. 4; (c) B. Kräutler and J. Maynollo, Diels-Alder reactions of the [60]fullerene functionalizing a carbon sphere with flexibly and with rigidly bound addends, *Tetrahedron*, 1996, **52**, 5033–5042; (d) J. A. Schlueter, J. M. Seaman, S. Taha, H. Cohen, K. R. Lykke, H. H. Wang and J. M. Williams, Synthesis, purification, and characterization of the 1:1 addition product of C<sub>60</sub> and anthracene, *J. Chem. Soc., Chem. Commun.*, 1993, 972–974.
- 6 (a) M. Yamada, R. Ochi, Y. Yamamoto, S. Okada and Y. Maeda, Transition-metal-catalyzed divergent functionalization of [60]fullerene with propargylic esters, *Org. Biomol. Chem.*, 2017, **15**, 8499–8503; (b) M. Yamada, A. Ishitsuka, Y. Maeda, M. Suzuki and H. Sato, Copper-mediated cascade synthesis of open-cage fullerenes, *Org. Lett.*, 2020, **22**, 3633–3636; (c) T. Muraoka, H. Asaji, Y. Yamamoto, I. Matsuda and K. Itoh, Rhodium-catalyzed silylative carbocyclization on C<sub>60</sub>, *Chem. Commun.*, 2000, 199–200; (d) S.-P. Jiang, W.-Q. Lu, Z. Liu and G.-W. Wang, Synthesis of fullerotetrahydroquinolines via [4 + 2] cycloaddition reaction of [60]fullerene with in situ generated aza-quinone methides, *J. Org. Chem.*, 2018, **83**, 1959–1968; (e) S.-P. Jiang, Z. Liu, W.-Q. Lu and G.-W. Wang, Synthesis of fullerotetrahydropyridazines via the copper-catalyzed heteroannulation of [60]fullerene with hydrazides, *Org. Chem. Front.*, 2018, **5**, 1188–1193; (f) A. Artigas, J. Vila, A. Lledó, M. Solà, A. Pla-Quintana and A. Roglans, A Rh-catalyzed cycloisomerization/Diels-Alder cascade reaction of 1,5-bisallenes for the synthesis of polycyclic heterocycles, *Org. Lett.*, 2019, **21**, 6608–6613; (g) A. Artigas, C. Castanyer, N. Roig, A. Lledó, M. Solà, A. Pla-Quintana and A. Roglans, Synthesis of fused dihydroazapeine derivatives of fullerenes by a Rh-catalyzed cascade process, *Adv. Synth. Catal.*, 2021, **363**, 3835–3844; (h) C. Castanyer, A. Artigas, N. Insa-Carreras, M. Solà, A. Pla-Quintana and A. Roglans, Rh-catalyzed cycloaddition of C<sub>60</sub> with enynes: unveiling the mechanistic pathway, *Adv. Synth. Catal.*, 2024, **366**, 862–869; (i) C. Castanyer, A. Artigas, M. Solà, A. Pla-Quintana and A. Roglans, On the functionalization of C<sub>60</sub> with vinylallenes generated in situ by rhodium catalysis, *Adv. Synth. Catal.*, 2025, **367**, e202401163; (j) W. Duzcek, W. Radeck, H.-J. Niclas, M. Ramm and B. Costisella, Diels-Alder cycloaddition of substituted norcaradienes with [60]fullerene, *Tetrahedron Lett.*, 1997, **38**, 6651–6654.
- 7 G. Pareras, S. Simon, A. Poater and M. Solà, Successive Diels-Alder cycloadditions of cyclopentadiene to [10]CPP ⊂ C<sub>60</sub>: a computational study, *J. Org. Chem.*, 2022, **87**, 5149–5157.
- 8 I. Lamparth and A. Hirsch, Water-soluble malonic acid derivatives of C<sub>60</sub> with a defined three-dimensional structure, *Chem. Commun.*, 1994, 1727–1728.
- 9 (a) L. L. Dugan, D. M. Turetsky, C. Du, D. Lobner, M. Wheeler, C. R. Almlı, C. K.-F. Shen, T.-Y. Luh, D. W. Choi and T.-S. Lin, Carboxyfullerenes as neuroprotective agents, *Proc. Natl. Acad. Sci. U. S. A.*, 1997, **94**, 9434–9439; (b) S. S. Ali, J. I. Hardt, K. L. Quick, J. Sook Kim-Han, B. F. Erlanger, T. T. Huang, C. J. Epstein and L. L. Dugan, A biologically effective fullerene (C<sub>60</sub>) derivative with superoxide dismutase mimetic properties, *Free Radical Biol. Med.*, 2004, **37**, 1191–1202.
- 10 (a) U. Hahn, F. Vögtle and J.-F. Nierengarten, Synthetic strategies towards fullerene-rich dendrimer assemblies, *Polymers*, 2012, **4**, 501–538; (b) J.-F. Nierengarten, Fullerene hexa-adduct scaffolding for the construction of giant molecules, *Chem. Commun.*, 2017, **53**, 11855–11868.
- 11 T. Cao, F. Wei, Y. Yang, L. Huang, X. Zhao and W. Cao, Microtribologic properties of a covalently attached nanostructured self-assembly film fabricated from fullerene carboxylic acid and diazoresin, *Langmuir*, 2002, **18**, 5186–5189.
- 12 (a) C. Thilgen, S. Sergeev and F. Diederich, Spacer-controlled multiple functionalization of fullerenes, *Top. Curr. Chem.*, 2004, **248**, 1–61; (b) C. Thilgen and F. Diederich, Tether-directed remote functionalization of fullerenes C<sub>60</sub> and C<sub>70</sub>, *C. R. Chim.*, 2006, **9**, 868–880.
- 13 (a) L. Isaacs, R. F. Haldimann and F. Diederich, Tether-directed remote functionalization of buckminsterfullerene: regiospecific hexaadduct formation, *Angew. Chem., Int. Ed. Engl.*, 1994, **33**, 2339–2342; (b) F. Cardullo, P. Seiler, L. Isaacs, J.-F. Nierengarten, R. E. Haldimann, F. Diederich, T. Mordasini-Denti, W. Thiel, C. Boudon, J.-P. Gisselbrecht and M. Gross, Bis- through tetrakis-adducts of C<sub>60</sub> by reversible tether-directed remote functionalization and systematic investigation of the changes in fullerene properties as a function of degree, pattern, and nature of functionalization, *Helv. Chim. Acta*, 1997, **80**, 343–371.
- 14 (a) W. Qian and Y. Rubin, Towards sixfold functionalization of Buckminsterfullerene (C<sub>60</sub>) at fully addressable octahedral sites, *Angew. Chem., Int. Ed.*, 1999, **38**, 2356–2360; (b) S.-C. Chuang, S. I. Khan and Y. Rubin, Switch of electronic reactivity in fullerene C<sub>60</sub>: activation of three *trans*-4



- positions via temporary saturation of the *cis*-1 positions, *Org. Lett.*, 2006, **8**, 6075–6078.
- 15 (a) G. Rapenne, J. Crasouos, A. Collet, L. Echegoyen and F. Diederich, Regioselective one-step synthesis of *trans*-3, *trans*-3,*trans*-3 and *e,e,e*, [60]fullerene tris-adducts directed by a C<sub>3</sub>-symmetrical cyclotrimeratrylene tether, *Chem. Commun.*, 1999, 1121–1122; (b) U. Reuther, T. Brandmüller, W. Donaubauer, F. Hampel and A. Hirsch, A highly regioselective approach to multiple adducts of C<sub>60</sub> governed by strain minimization of macrocyclic malonate addends, *Chem. – Eur. J.*, 2002, **8**, 2261–2273; (c) F. Beuerle, N. Chronakis and A. Hirsch, Regioselective synthesis and zone selective deprotection of [60]fullerene tris-adducts with an *e,e,e* addition pattern, *Chem. Commun.*, 2005, 3676–3678; (d) F. Beuerle and A. Hirsch, Synthesis and orthogonal functionalization of [60]fullerene *e,e,e*-trisadducts with two spherically defined addend zones, *Chem. – Eur. J.*, 2009, **15**, 7434–7446; (e) A. Kraszewska, P. Rivera-Fuentes, G. Rapenne, J. Crassous, A. G. Petrovic, J. L. Alonso-Gómez, E. Huerta, F. Diederich and C. Thilgen, Regioselectivity in tether-directed remote functionalization – the addition of a cyclotrimeratrylene-based trimalonate to C<sub>60</sub> revisited, *Eur. J. Org. Chem.*, 2010, 4402–4411; (f) A. Gmehling, W. Donaubauer, F. Hampel, F. W. Heinemann and A. Hirsch, Invertomers of fullerene-phosphates, *Angew. Chem., Int. Ed.*, 2013, **52**, 3521–3524; (g) S. Guerra, F. Schillinger, D. Sigwalt, M. Holler and J.-F. Nierengarten, Synthesis of optically pure [60]fullerene *e,e,e*-tris adducts, *Chem. Commun.*, 2013, **49**, 4752–4754; (h) D. Sigwalt, F. Schillinger, S. Guerra, M. Holler, M. Berville and J.-F. Nierengarten, An expeditious regioselective synthesis of [60]fullerene *e,e,e* tris-adduct building blocks, *Tetrahedron Lett.*, 2013, **54**, 4241–4244; (i) M. Wachter, L. Jurkiewicz and A. Hirsch, Sequential tether-directed synthesis of new [3 : 2 : 1] hexakis-adducts of C<sub>60</sub> with a mixed octahedral addition pattern, *Chem. – Eur. J.*, 2021, **27**, 7677–7686; (j) E. Meichsner, F. Schillinger, T. M. N. Trinh, S. Guerra, U. Hahn, I. Nierengarten, M. Holler and J.-F. Nierengarten, Regioselective synthesis of fullerene tris-adducts for the preparation of clickable fullerene [3 : 3]-hexa-adduct scaffolds, *Eur. J. Org. Chem.*, 2021, 3787–3797.
- 16 (a) C. Fuertes-Espinosa, C. García-Simón, M. Pujals, M. Garcia-Borràs, L. Gómez, T. Parella, J. Juanhuix, I. Imaz, D. Maspoch, M. Costas and X. Ribas, Supramolecular fullerene sponges as catalytic masks for regioselective functionalization of C<sub>60</sub>, *Chem*, 2020, **6**, 169–186; (b) M. Pujals, T. Pèlachs, C. Fuertes-Espinosa, T. Parella, M. Garcia-Borràs and X. Ribas, Regioselective access to orthogonal Diels-Alder C<sub>60</sub> bis-adducts and tris-adducts via supramolecular mask strategy, *Cell Rep. Phys. Sci.*, 2022, **3**, 100992; (c) V. Iannace, C. Sabrià, Y. Xu, M. von Delius, I. Imaz, D. Maspoch, F. Feixas and X. Ribas, Regioswitchable Bingel bis-functionalization of Fullerene C<sub>70</sub> via supramolecular masks, *J. Am. Chem. Soc.*, 2024, **146**, 5186–5194; (d) T. Pèlachs, C. Sabrià, V. Iannace, I. Imaz, F. Gándara, D. Maspoch, F. Feixas and X. Ribas, Supramolecular mask regioconverter: orthogonal Diels-Alder C<sub>70</sub> bisadducts by mask-mediated regioselective synthesis, *CCS Chem.*, 2025, **7**, 703–715.
- 17 (a) A. Kinoshita and M. Mori, Ruthenium catalyzed enyne metathesis, *Synlett*, 1994, 1020–1022; (b) M. Mori, N. Sakakibara and A. Kinoshita, Remarkable effect of ethylene gas in the intramolecular enyne metathesis of terminal alkynes, *J. Org. Chem.*, 1998, **63**, 6082–6083; (c) D. Bentz and S. Laschat, Synthesis of perhydroindenes and perhydroisindoles via one-pot enyne metathesis/Diels-Alder reaction; remarkable stability of Grubbs catalyst under Lewis acidic conditions, *Synthesis*, 2000, 1766–1773; (d) H.-Y. Lee, H. Y. Kim, H. Tae, B. G. Kim and J. Lee, One-pot three-component tandem metathesis/Diels-Alder reaction, *Org. Lett.*, 2003, **5**, 3439–3442; For general reviews, see: (e) Y. Yamamoto, Recent topics of Cp/RuCl-catalyzed annulation reactions, *Tetrahedron Lett.*, 2017, **58**, 3787–3794; (f) Y. Hu, M. Bai, Y. Yang and Q. Zhou, Metal-catalyzed enyne cycloisomerization in natural product total synthesis, *Org. Chem. Front.*, 2017, **4**, 2256–2275; (g) E. Jiménez-Núñez and A. M. Echavarren, Gold-catalyzed cycloisomerizations of enynes: A mechanistic perspective, *Chem. Rev.*, 2008, **108**, 3326–3350; (h) V. Michelet, P. Y. Toullec and J.-P. Genêt, Cycloisomerization of 1,*n*-enyne: challenging metal-catalyzed rearrangements and mechanistic insights, *Angew. Chem., Int. Ed.*, 2008, **47**, 4268–4315.

